

# Thickness of Hydroxyapatite Nanocrystal Controls Mechanical Properties of the Collagen–Hydroxyapatite Interface

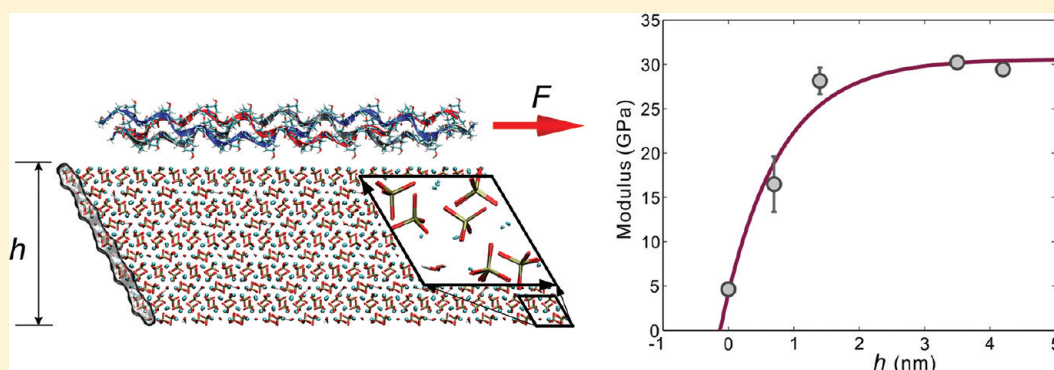
Zhao Qin,<sup>†</sup> Alfonso Gautieri,<sup>†,‡</sup> Arun K. Nair,<sup>†</sup> Hadass Inbar,<sup>†</sup> and Markus J. Buehler<sup>\*,†,§,||</sup>

<sup>†</sup>Laboratory for Atomistic and Molecular Mechanics (LAMM), Department of Civil and Environmental Engineering, Massachusetts Institute of Technology, 77 Massachusetts Avenue, Room 1-235 A&B, Cambridge, Massachusetts 02139, United States

<sup>‡</sup>Biomechanics Research Group, Department of Bioengineering, Politecnico di Milano, Via Golgi 39, 20133 Milan, Italy

<sup>§</sup>Center for Computational Engineering, Massachusetts Institute of Technology, 77 Massachusetts Avenue, Cambridge, Massachusetts 02139, United States

<sup>||</sup>Center for Materials Science and Engineering, Massachusetts Institute of Technology, 77 Massachusetts Avenue, Cambridge, Massachusetts 02139, United States



**ABSTRACT:** Collagen–hydroxyapatite interfaces compose an important building block of bone structures. While it is known that the nanoscale structure of this elementary building block can affect the mechanical properties of bone, a systematic understanding of the effect of the geometry on the mechanical properties of this interface between protein and mineral is lacking. Here we study the effect of geometry, different crystal surfaces, and hydration on the mechanical properties of collagen–hydroxyapatite interfaces from an atomistic perspective, and discuss underlying deformation mechanisms. We find that the presence of hydroxyapatite significantly enhances the tensile modulus and strength compared with a tropocollagen molecule alone. The stiffening effect is strongly dependent on the thickness of the mineral crystal until a plateau is reached at 2 nm crystal thickness. We observe no significant differences due to the mineral surface (Ca surface vs OH surface) or due to the presence of water. Our result shows that the hydroxyapatite crystal with its thickness confined to the nanometer size efficiently increases the tensile modulus and strength of the collagen–hydroxyapatite composite, agreeing well with experimental observations that consistently show the existence of extremely thin mineral flakes in various types of bones. We also show that the collagen–hydroxyapatite interface can be modeled with an elastic network model which, based on the results of atomistic simulations, provides a good estimate of the surface energy and other mechanical features.

## 1. INTRODUCTION

Bone serves a variety of mechanical, synthetic, and metabolic functions in the body.<sup>1</sup> This tough, lightweight, elastic, and highly dissipative material acts as a protective load-bearing framework and shows remarkable mechanical properties. Bone has two main constituents: collagen protein and apatite mineral.<sup>2,3</sup> Collagen molecules assemble into fibrils, which mineralize by the formation of mineral crystals in the gap regions that exist due to the staggered arrangement, as shown in Figure 1a. Mineralized collagen fibrils form higher-level hierarchical structures of bone by assembling with extrafibrillar matrix. While larger structures differ depending on bone type, structures of mineralized fibrils are highly conserved across

species and different types of bone, and act as bone's universal elementary building block.<sup>4–7</sup>

There are several forms of apatites, with the general formula  $\text{Ca}_{10}(\text{PO}_4)_6\text{X}_2$  where X can be F, Cl, Br, or OH. The latter is the case of hydroxyapatite (HA), the most relevant apatite in bone. Bone hydroxyapatite is in the form of nanosized mineral platelets, where the thickness of the platelets can range from 1 to 7 nm, the length from 15 to 200 nm, and the width from 10

**Special Issue:** Bioinspired Assemblies and Interfaces

**Received:** October 16, 2011

**Revised:** December 26, 2011

**Published:** December 31, 2011

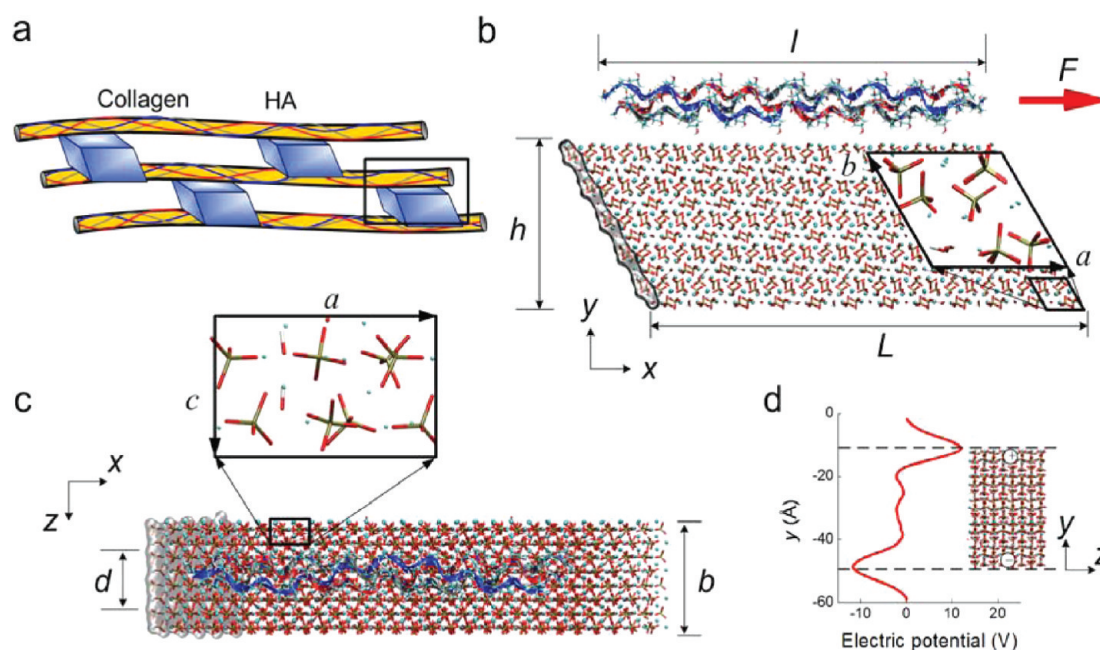


**Figure 1.** Schematic of the molecular systems studied here. Panel a shows a schematic arrangement of the assembly of tropocollagen molecule and hydroxyapatite crystals in the bone. We focus on the region selected by black rectangular as shown. Panel b shows a lateral view and boundary conditions of the systems with collagen molecule lying on the Ca surface. A lateral total force  $F$  that is parallel to the surface in the  $x$ -direction is applied to the three  $\alpha$  carbon atoms at the right end of the tropocollagen segment, while a single layer of atoms at the left end of the hydroxyapatite is fixed as shown by the transparent glue. The OH surface is the bottom surface of the hydroxyapatite crystal in this panel. We zoom in to show the projection of a unit cell of the hydroxyapatite with its two lattice constant  $a$  and  $b$ . Panel c shows a top view of the system. We zoom in to show the projection of a unit cell of the hydroxyapatite with its two lattice constant  $a$  and  $c$ . Panel d shows the electric potential across the hydroxyapatite crystal in the thickness direction (in  $y$ -direction) showing the negative nature of the OH surface and the positive nature of Ca surface.

**Table 1. Basic Geometric and Mechanical Properties of Tropocollagen Molecule and Hydroxyapatite**

material	crystal type	geometric parameters	basic unit	method of mechanical test	tensile modulus (GPa)	extensibility	tensile strength (GPa)
tropocollagen molecule	protein triple helix	$d = 1.5$ nm $l = 9.3$ nm	GPO	experiment <sup>45</sup> simulation <sup>27</sup>	0.35–12 1.8–4	30% 50%	13
hydroxyapatite	hexagonal crystal	$h = 0.7$ – $4.2$ nm $b = 2.5$ nm $L = 10.5$ nm	$\text{Ca}_{10}(\text{PO}_4)_6(\text{OH})_2$	experiment <sup>46</sup> simulation <sup>12</sup>	114 120.6	10%–16%	7.4–9.6

to 80 nm.<sup>4,5,7,8</sup> The differences of geometric and mechanical properties of the collagen fibrils and hydroxyapatite crystals are distinct. Collagen fibrils are soft and ductile, while the bulk hydroxyapatite is stiff and brittle, as summarized in Table 1. The geometric characteristic of a typical model of these two materials in human bone structures are as summarized in Figure 1.

Collagen–hydroxyapatite composites are not only the basic building blocks of human bone, but they are among the most abundant class of biomineralized materials in the animal kingdom. This composite exhibits properties of both hard and soft matter, combining the toughness of inorganic material and the flexibility of biological tissues. Although the structure of bone and its mechanical properties are well-studied, the knowledge about how collagen fibrils and hydroxyapatite crystals interact and deform as an integrated system under external stress are not well understood. Indeed, despite collagen being a soft material and hydroxyapatite being brittle, combined they form a composite of high-mechanical strength and fracture toughness.<sup>8</sup> A deep understanding of the properties of bone building blocks requires a thorough investigation of the interplay of the organic molecules with the mineral crystals.

Therefore, how the mechanical property of collagen–hydroxyapatite interface follows the morphology of the crystals becomes critical in understanding the mechanism of the bone's superior mechanical property at the most fundamental level. Understanding of this mechanism is important to model the composites from the bottom up. This, in turn, requires an atomistic-level investigation of the chemo-mechanical properties of the organic–inorganic interfaces and its correlation with the overall mechanical behavior of the composite materials.

Molecular simulation approaches may achieve the atomistic resolution needed for such detailed mechanistic analyses and investigate biomineral interfaces at a level that is still difficult or impossible to achieve with experimental techniques alone. Nonetheless, atomistic simulation studies of hydroxyapatite are relatively recent, initially concentrating on the pure material.<sup>9,10</sup> Subsequently, atomistic simulations have also been used to gain insights into the mechanical properties of hydroxyapatite<sup>11–13</sup> and its interface with proteins and peptides.<sup>14–16</sup> Of particular interest for the present study is the interaction of hydroxyapatite with tropocollagen molecules, which is the major protein phase in bone and thus understanding its interaction with hydroxyapatite is critical. Previous works have

used atomistic simulations to investigate the load-deformation behavior of tropocollagen molecules with hydroxyapatite in the proximity of their terminals,<sup>17,18</sup> the adsorption energy of tropocollagen molecules such as the common Gly-Pro-Hyp segment,<sup>19,20</sup> and the modeling of nanosystems that mimic mineralized fibrils<sup>21,22</sup> or enamel.<sup>23</sup> In atomistic modeling, all the interactions between tropocollagen molecule and hydroxyapatite at interfaces are decomposed into basic terms including van der Waals interactions, Coulombic interactions, and hydrogen bonds.<sup>24</sup> The van der Waals interaction is pairwise for all the atom pairs in the tropocollagen molecule and hydroxyapatite, while the Coulombic interactions mainly exist between charged side-chains (e.g.,  $\text{NH}_3^+$  and  $\text{COO}^-$ ) and surface ions of hydroxyapatite ( $\text{Ca}^{2+}$ ,  $\text{PO}_4^{3-}$ ,  $\text{OH}^-$ ). Hydrogen bonds were formed between the uncharged polar side-chains (e.g., OH in Hyp) and OH groups in hydroxyapatite. Although those studies are helpful in revealing the adhesive properties at the mineral surface, none of the earlier works provided direct evidence to reveal the morphology–function relationship of the collagen–hydroxyapatite composite at the nanoscopic scale.

**Research Design.** In order to investigate the nanomechanics of the collagen–hydroxyapatite interface, in this work we examine the mechanical properties (such as the tensile modulus and the tensile strength) of a tropocollagen molecule at the interface of hydroxyapatite. For this purpose, we perform a series of *in silico* mechanical tests by loading a tropocollagen molecule lying on a hydroxyapatite substrate and assessing the forces and investigating the details of deformation mechanisms. A further aim of the work is to investigate how the interface properties, such as the thickness of the hydroxyapatite substrate, the hydroxyapatite surface type (Ca surface versus OH surface), and the hydration state, influence the nanomechanics of the collagen–hydroxyapatite interface. Our molecular simulation enables the visualization of the stress distribution within tropocollagen molecules and hydroxyapatite under mechanical loading, which helps us to identify the molecular mechanism that governs the deformation of tropocollagen molecule at the collagen–hydroxyapatite interface. This allows for a deeper understanding of the structure–function relationship of the bone and can facilitate bottom-up material design of synthetic bone materials with optimized material properties or potentially an improved understanding of bone disease. The solvent condition is very important in conserving the protein conformation by stabilizing its secondary structure. However, it is unclear whether the hydration condition can alter the thickness effect and how much difference it can cause. To explore this issue, we include a comparison between the simulations in dry and in solvated conditions.

## 2. METHODS

**Atomic Model of Tropocollagen Molecule and Hydroxyapatite.** We build the model of the tropocollagen molecule by using the software THeBuScr (Triple Helical Collagen Building Script),<sup>25</sup> which has been applied before in modeling the tropocollagen molecule.<sup>26</sup> We choose the simplest model of collagen, with only Gly-Pro-Hyp triplets on each of the three chains. The tropocollagen molecule model we use, [(Gly-Pro-Hyp)<sub>10</sub>]<sub>3</sub>, is truncated to 30 amino acids per chain in order to reduce computational costs, since peptides of comparable length have been used in previous studies.<sup>27,28</sup> Because the tropocollagen length (9 nm) is much shorter than its persistence length (10–20 nm), entropic effects are not considered here. The computational model is developed with the aim of elucidating the generic behavior and deformation of a system containing a single

tropocollagen molecule and a crystal of hydroxyapatite, and as such is designed to be simple and not intended to be a direct representation of the actual bone nanostructure. However, it enables us to perform a systematic study of bone nanomechanics from a fundamental point of view. The geometry and characteristics of the simulation system are shown in Figure 1.

**Tropocollagen Parametrization.** Collagen is the sole protein that features hydroxyproline (HYP), a nonstandard amino acid, resulting from hydroxylation of proline. Since it is rarely found, HYP is not parametrized in common biomolecular force fields such as CHARMM.<sup>29</sup> However, a set for HYP has been developed by using quantum mechanics simulations and subsequently deriving the atomistic parameters that best match the quantum-mechanics calculation,<sup>30</sup> with particular focus on the correct modeling of the pucker of the HYP ring. These parameters have been then successfully used for collagen modeling in previous works.<sup>28,31,32</sup>

**Hydroxyapatite Force Field Parametrization.** Most force fields for biomolecular simulation, like CHARMM,<sup>29</sup> do not include parameters for mineral crystal such as hydroxyapatite. Therefore, in order to model biomolecular systems including hydroxyapatite, we extended the CHARMM force field. We use bond, angle, and dihedral parameters as those reported earlier,<sup>10</sup> which are based on both quantum-mechanics calculations and empirical data. For nonbonded parameters, the authors adopted a Born–Mayer–Huggins model, which is not available in the CHARMM force field. Therefore, for nonbonded terms, we use data from ref 33 in which the authors fitted the Born–Mayer–Huggins potential<sup>10</sup> with a simpler Lennard-Jones potential. The parametrization of force field consisted of three consecutive stages:<sup>10</sup>

- Fitting of the site charges as to represent the quantum-chemically computed electrostatic field within the three-dimensional (3D) periodic crystal environment;
- Derivation of intramolecular phosphate parameters from gas-phase quantum-chemical calculations;
- Optimization of the remaining nonbonded parameters with respect to minimal deviations between computed and experimental crystal structures via molecular dynamics simulations.

**Crystal Geometry.** We generated the hexagonal hydroxyapatite crystal unit cell by using the Material Studio 4.4 (Accelrys, Inc.), which presents the following lattice parameters:  $a = 9.4214 \text{ \AA}$ ,  $b = 9.4214 \text{ \AA}$ ,  $c = 6.8814 \text{ \AA}$ ,  $\alpha = 90^\circ$ ,  $\beta = 90^\circ$ , and  $\gamma = 120^\circ$ . On the basis of this unit cell (44 atoms per unit cell), hydroxyapatite crystals of varying thicknesses of 0.7 nm, 1.4 nm, 3.5 nm, and 4.2 nm are generated. We focus on the interaction on the (010) plane because this plane is dominant in the morphology of the biological material, due to the growth-directing effect of the collagen matrix.<sup>24</sup> Another reason we study this plane is that the electrostatic characteristic for the two opposite surfaces of this plane is not neutral but negative of the OH surface and positive of the Ca surface, as shown in Figure 1d. Since the interaction between the tropocollagen molecule and mineral part is basically composed of van der Waals interactions, electrostatic interactions, and hydrogen bonds, those two surfaces provide two extreme cases for validating our conclusions. Because the (100) plane has similar geometric and chemical properties as the (010) plane and the (001) plane is neutral, the conclusions of the thickness effect in the paper are valid for both those surfaces.

**Molecular Dynamics Simulations.** Molecular dynamics calculations are performed using LAMMPS code<sup>34</sup> and the modified CHARMM force field. Lennard-Jones and Coulomb interactions are computed with a switching function that ramps the energy and force smoothly to zero starting with 8 Å and cutting off at 10 Å. This cutoff range is selected to include at least one complete lattice in the thickness direction. We have tested cutoff lengths longer than this value and the tensile modulus and strength of the collagen–hydroxyapatite model are not affected by this increment. The constructed collagen–hydroxyapatite model is first geometrically optimized through energy minimization, then an NVT equilibration



**Table 2.** Values of the Parameters of the Tensile Modulus and Strength of Collagen–Hydroxyapatite Interfaces as a Function of the Thickness of the Hydroxyapatite, Given by Eqs 6 and 7<sup>a</sup>

parameter	surface 1 (calcium)		surface 2 (hydroxy)	
	no water	with water	no water	with water
$E_{\infty}$ (GPa)	30.16	31.72	31.72	31.87
$h_0$ (nm)	0.86	0.51	0.02	0.36
$\sigma_{\infty}$ (GPa)	20.79	21.41	19.37	20.62
$h_t$ (nm)	0.84	0.68	0.02	0.60
H-bonds at collagen–hydroxyapatite interface of $\varepsilon < 0.75$ (/nm)	$0.6 \pm 0.08$	$0.5 \pm 0.1$	$1.04 \pm 0.13$	$1.02 \pm 0.2$
H-bonds at collagen–hydroxyapatite interface of $\varepsilon > 0.75$ until rupture (/nm)	$0.6 \pm 0.2$	$0.2 \pm 0.13$	$0.94 \pm 0.1$	$0.8 \pm 0.35$

<sup>a</sup>The hydrogen bond density at the collagen–hydroxyapatite interfaces (for  $h = 1.4$  nm) are summarized here.

is performed for 200 ps. The system temperature is set to 300 K with Langevin thermostat. After the equilibration, we observe that the root-mean-square deviation of the crystal is stable, and that no major changes occur in the crystal structure, confirming the reliability of the extended CHARMM force field. We use steered molecular dynamics (SMD) for loading, constraining the left-end part of the hydroxyapatite crystal, and pulling the center of mass of the terminal  $\alpha$ -carbon on the tropocollagen molecule right-end (see Figure 1b). The pulling velocity is set to 0.01 Å/ps (1 m/s), similar to that used in previous studies of the proteins' tensile properties.<sup>28,35–37</sup>

**Visualization and Data Analysis.** We use visual molecular dynamics (VMD)<sup>38</sup> to show the snapshots of simulation and compute hydrogen bonds. We count the hydrogen bonds within a cutoff distance of 3.5 Å and an angle range of 30°. We use MATLAB (Mathworks, Inc.) to analyze the results of the mechanical response under tension. We keep a record of the applying force  $F$  as a function of the displacement of the SMD loading point  $dx$ . In the postprocessing stage, we calculate the applied stress to the end of the tropocollagen molecule via  $\sigma = F/A$  where  $A = \pi D^2/4$  is the cross-section area of the tropocollagen molecule, where  $D$  is the average diameter. Here  $A$  only counts the cross-section of the tropocollagen molecule because the force in our model is directly applied to the tropocollagen molecule end for the simulation set up. The tensile deformation is measured by the engineering strain calculated via  $\varepsilon = dx/l$  where  $l$  is the length of the tropocollagen molecule. We fit the  $\sigma$ – $\varepsilon$  curve for deformation up to 5% strain against a linear function to find the slope of the  $\sigma$ – $\varepsilon$  curve at the zero deformation, which yields the value of the tensile modulus  $E = d\sigma/d\varepsilon|_{\varepsilon=0}$ . We repeat the linear fit procedure for the  $\sigma$ – $\varepsilon$  curve for deformation up to 8% strain to find the tensile modulus as  $E'$  and then obtain the height of the error bars as  $|E - E'|$  for the tensile modulus.

**Elastic Network Model.** The deformation of the network can be obtained by solving the equation

$$K_{ij}X_j = F_i \quad (1)$$

where  $X$  is the vector of the displacement of each discrete point in the model,  $F$  is the force vector of the external force at each point, and the stiffness matrix  $K$  of the system is given by

$$K = \begin{bmatrix} K_{11(n \times n)} & K_{12(n \times n)} \\ K_{21(n \times n)} & K_{22(n \times n)} \end{bmatrix}_{(2n \times 2n)} \quad (2)$$

where  $K_{11}$ ,  $K_{12}$ ,  $K_{21}$ , and  $K_{22}$  are submatrices of the size  $n \times n$ . Here  $n$  is the number of nodes in the tensile direction, with a value of  $n = l/\Delta l$ , where  $\Delta l$  is the unit length between the two nodes. Each of the matrices is of the expression as

$$K_{11(n \times n)} = \begin{bmatrix} k_1 + k_3 & -k_1 & 0 & \dots & 0 & 0 \\ -k_1 & 2k_1 + k_3 & -k_1 & 0 & \dots & 0 \\ & & \dots & & & \\ 0 & 0 & 0 & \dots & -k_1 & 2k_1 + k_3 & -k_1 \\ 0 & 0 & 0 & \dots & 0 & -k_1 & k_1 + k_3 \end{bmatrix}_{(n \times n)} \quad (3)$$

$$K_{12(n \times n)} = K_{21(n \times n)} = \begin{bmatrix} -k_3 & 0 & 0 & \dots & 0 & 0 \\ 0 & -k_3 & 0 & \dots & 0 & 0 \\ & & \dots & & & \\ 0 & 0 & 0 & \dots & -k_3 & 0 \\ 0 & 0 & 0 & \dots & 0 & -k_3 \end{bmatrix}_{(n \times n)} \quad (4)$$

$$K_{22(n \times n)} = \begin{bmatrix} k_2 + k_3 & -k_2 & 0 & \dots & 0 & 0 \\ -k_2 & 2k_2 + k_3 & -k_2 & 0 & \dots & 0 \\ & & \dots & & & \\ 0 & 0 & 0 & \dots & -k_2 & 2k_2 + k_3 & -k_2 \\ 0 & 0 & 0 & \dots & 0 & -k_2 & \infty \end{bmatrix}_{(n \times n)} \quad (5)$$

where  $K_{2n,2n} = \infty$  corresponds to the fixed boundary condition. Each of the elastic parameters  $k_1$ ,  $k_2$ , and  $k_3$  represents the tensile modulus of the tropocollagen molecule, hydroxyapatite, and the interfacial interaction (including all nonbonded interactions, i.e., the van der Waals interactions, the Coulomb interactions, and hydrogen bonds), respectively. We have  $k_1 = E_{\text{COL}}A_{\text{COL}}/\Delta l$  and  $k_2 = E_{\text{HA}}A_{\text{HA}}/\Delta l$ , where  $E_{\text{COL}}$  and  $E_{\text{HA}}$  are the tensile modulus of the tropocollagen molecule and hydroxyapatite, respectively and  $A_{\text{COL}}$  and  $A_{\text{HA}}$  are the cross-section area of the tropocollagen molecule and hydroxyapatite, respectively. For our model, we have  $A_{\text{COL}} = \pi D^2/4$  and  $A_{\text{HA}} = bh$ , which is a function of the hydroxyapatite thickness. The values of those parameters are as summarized in Table 3. The value of the parameter  $k_3$  is unknown in the model, but we find its value by comparing the theoretical result to the simulation results.

The force boundary condition is included by using  $F = [F_{\text{app}} \ 0 \ 0 \ \dots \ 0 \ 0]^T_{(2n \times 1)}$ . On the basis of these conditions and parameters, we obtain the deformation of each node in the model as  $X_j$ , we find the deformation exponentially decreases from the point under tension to points further away. The tensile modulus of the entire model is calculated via  $E = F_{\text{app}}/l/(A_{\text{COL}}X_{j=1})$  in the same way as it was done for the atomic simulations. It is noted that the value of  $F_{\text{app}}$  used here does not affect the result because of each component in this tensile modulus is ideally elastic. Thereby, for any  $k_3$  value, we can obtain a corresponding curve for the tensile modulus–thickness relationship.

**Table 3. Values of the Parameters Used in the Elastic Network Model in This Study**

parameters	values
tropocollagen molecule diameter $D$ (in nm)	1.5
length of tropocollagen molecule $l$ (in nm)	9.0
width of HA $b$ (in nm)	2.5
unit length between nodes $\Delta l$ (in nm)	1.0
rupture distance of nonbonded interaction $\Delta x$ (in nm)	1.0
tensile modulus of tropocollagen molecule $E_{\text{COL}}$ (in GPa)	4.64
tensile modulus of hydroxyapatite nanocrystal $E_{\text{HA}}$ (in GPa)	120.6

### 3. RESULTS AND DISCUSSION

Using the models of tropocollagen molecule and hydroxyapatite as shown in Figures 1b–d, we study the effect of hydroxyapatite thickness  $h$  on the mechanical response of the model under applied force. The force–extension curves in our simulations corresponding to various thickness and chemical surfaces of the hydroxyapatite are summarized in Figure 2. All curves display a linear region from the beginning followed by a “bumpy” region before failure of the material occurs. We observe that the deformation of the model in the first region originates from the direct extension of the atomic interactions in the molecules, and rarely the sliding between the tropocollagen molecule and hydroxyapatite. For the “bumpy” region, we observe that the collagen chains, after fully stretching, starts to slide on top of the hydroxyapatite surface. Such a sliding mechanism occurs in a discontinuous way because of the atomically rough surface of the electrostatic interactions and hydrogen-bond-forming patterns. Figure 3 captures those characteristics by keeping a detailed record of the number of hydrogen bonds within the tropocollagen molecule as well as between the collagen and hydroxyapatite as a function of the deformation, measured by strain. We observe

an overall decreasing number of hydrogen bonds within the tropocollagen molecule from a number around 1.1 H-bond/nm to that around 0.7 H-bond/nm as summarized in Figure 3a–d (normalized by the equilibrated length of tropocollagen molecule which is 9.0 nm). We find that this trend is caused by the unfolding of the tropocollagen molecule, mediated by breaking of the interchain hydrogen bonds and increased alignment in the tension direction. From Figure 3e–h we further observe that the variation of the number of hydrogen bonds between tropocollagen and hydroxyapatite becomes significantly larger for the OH-terminated surface (the bottom surface of the crystal in Figure 1d). For example, for thickness  $h = 1.4$  nm on the Ca-terminated surface, we have a hydrogen bond number of  $0.6 \pm 0.08$  H-bond/nm for the linear region before the strain of 0.75, while the number becomes  $0.6 \pm 0.2$  H-bond/nm for the bumpy region beyond the strain of 0.75. On the OH surface, the average value is  $1.04 \pm 0.13$  H-bond/nm in the linear region, while it becomes  $0.94 \pm 0.1$  H-bond/nm in the second region. We observe that this trend is also found in the presence of water, where the number of hydrogen bonds between tropocollagen and hydroxyapatite is  $0.5 \pm 0.1$  H-bond/nm (linear region) and  $0.2 \pm 0.13$  H-bond/nm (bumpy region) for the Ca surface, whereas we find  $1.02 \pm 0.2$  H-bond/nm (linear region) and  $0.8 \pm 0.35$  H-bond/nm (bumpy region) for the OH surface. Such a difference in the average value and standard deviation agrees with what we can read from the vibrating force–extension curve and curve of hydrogen bond number between tropocollagen molecule and hydroxyapatite, which implies that the number of hydrogen bonds between tropocollagen molecule and hydroxyapatite contributes to the interaction force. All those results are summarized in Table 2.

We now investigate the thickness effect on the tensile modulus of the system for different surfaces and solvent

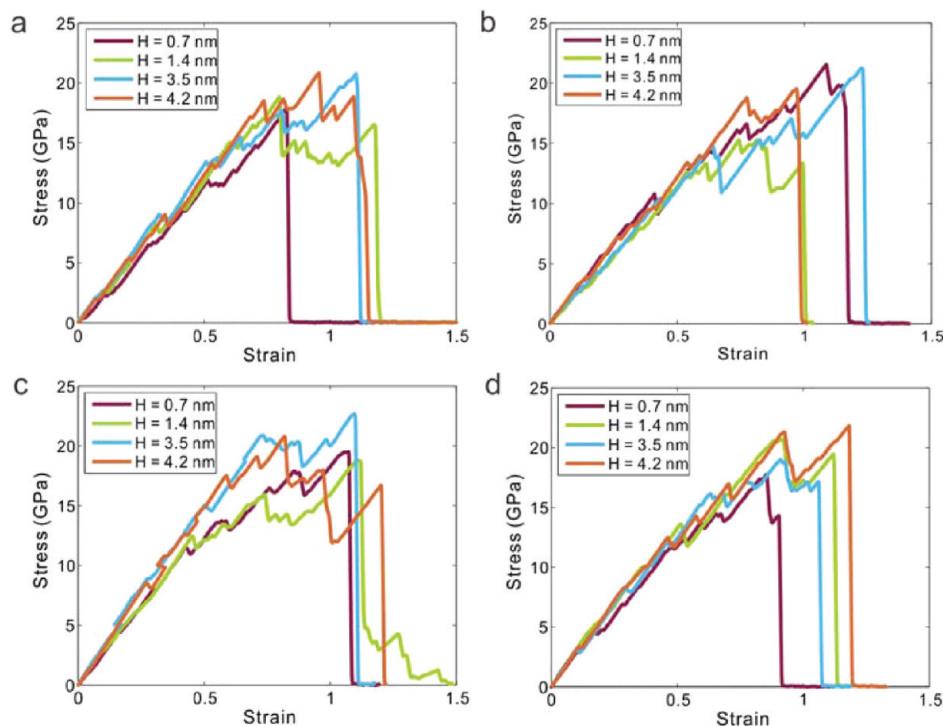


**Figure 2.** Stress–strain curves for collagen–hydroxyapatite composites. Stress–strain curves for Ca surface (a) and OH surface (b) in dry conditions, and Ca surface (c) and OH surface (d) in the presence of water.

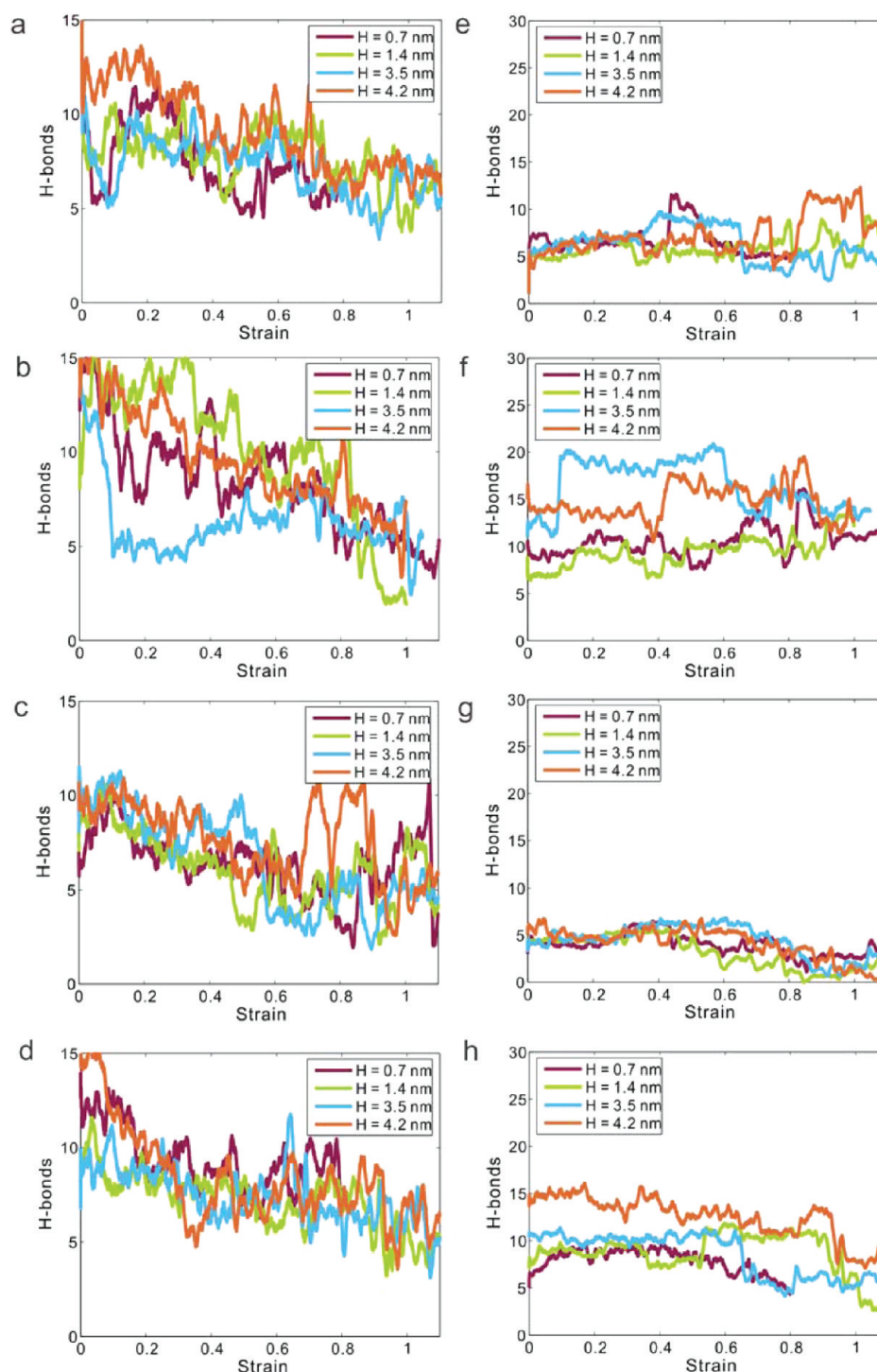


**Figure 3.** Number of hydrogen bonds. Panels a–d show the number of collagen intramolecular hydrogen bonds as a function of strain for the Ca surface in vacuum (a), the OH surface in vacuum (b), the Ca surface in water (c), and the OH surface in water (d). Panels e–h show the number of collagen–hydroxyapatite hydrogen bonds as a function of strain for the Ca surface in vacuum (e), the OH surface in vacuum (f), the Ca surface in water (g), and the OH surface in water (h).

conditions as summarized in Figure 4. It is observed that the existence of hydroxyapatite significantly increases the effective stiffness of the system by comparing the tensile modulus to that of the pure collagen triple helix (corresponding to the case  $h = 0$ ). The increasing tensile modulus as a function of the hydroxyapatite thickness decreases exponentially for  $h \neq 0$ , as shown in Figure 4. We fit those results mathematically by using the function

$$E = E_{\infty} - (E_{\infty} - E_{\text{COL}}) \exp(-h/h_0) \quad (6)$$

where  $E_{\infty}$  is the converged value of the tensile modulus for larger  $h$ ,  $E_{\text{COL}}$  (4.64 GPa for pure tropocollagen molecule stretching test in our simulation, which agrees with the result of an earlier simulation study<sup>28</sup>) is the tensile modulus of pure tropocollagen molecule, and  $h_0$  is a length constant as the characteristic thickness. It shows that for hydroxyapatite crystals

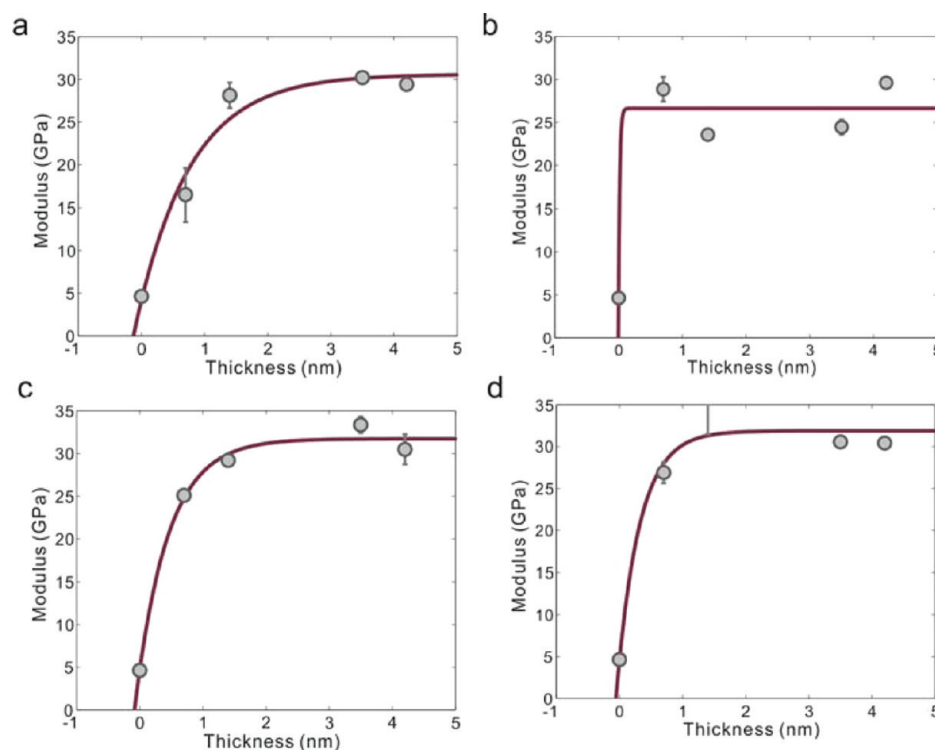


**Figure 4.** Effect of hydroxyapatite thickness on the tensile modulus. The tensile modulus of the collagen–hydroxyapatite system is shown as a function of the crystal thickness for the Ca surface in vacuum (a), the OH surface in vacuum (b), the Ca surface in water (c), and the OH surface in water (d).

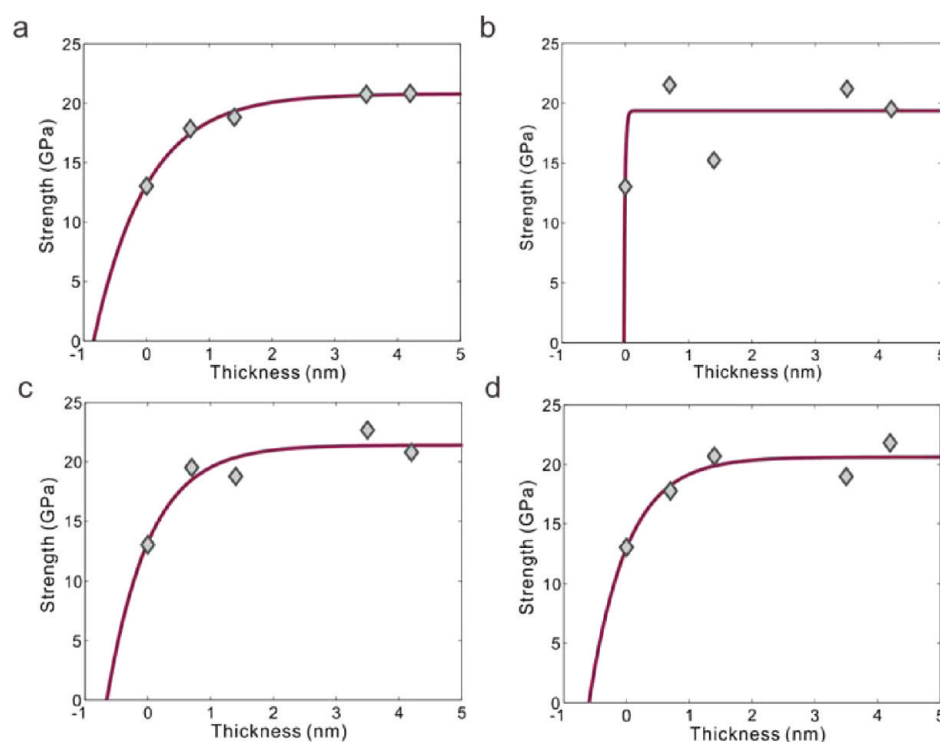


**Figure 5.** Effect of hydroxyapatite thickness on the tensile strength. The tensile strength, which corresponds to the maximum stress for the stress–strain curves as summarized in Figure 2, of the collagen–hydroxyapatite system is shown as a function of the crystal thickness for the Ca surface in vacuum (a), the OH surface in vacuum (b), the Ca surface in water (c), and the OH surface in water (d).

with a thickness beyond  $h_0$ , increasing the thickness can only increase the stiffness of the system up to 50%. We summarize  $E_\infty$  and  $h_0$  for each of the two surfaces with and without water around the interface in Table 2. It can be seen that  $E_\infty$  is rather

insensitive on the surface or hydration state, reaching a value of  $\sim 31$  GPa. On the other hand, the tensile modulus is shown to be dependent on the crystal thickness, in particular for the Ca surface in dry conditions, where the tensile modulus in the case



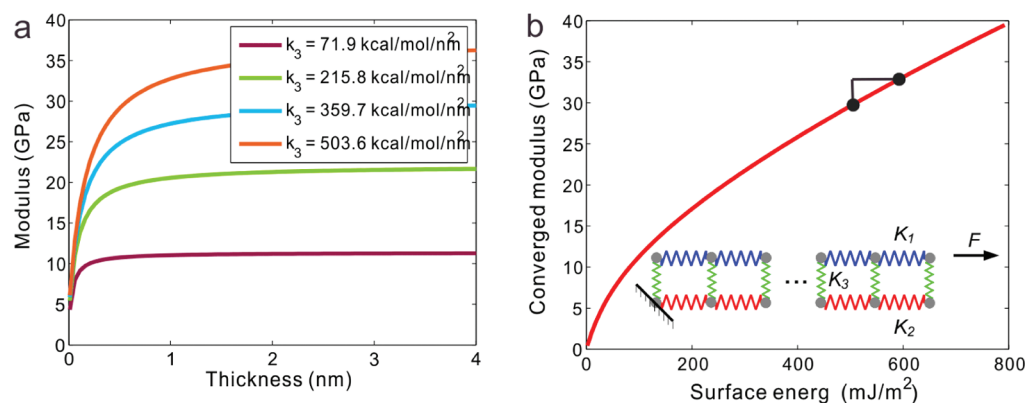


**Figure 6.** Elastic network model of tropocollagen molecule–hydroxyapatite interface. Panel a shows the tensile modulus–thickness relationship as a function of  $k_3$ , which represents the collagen–hydroxyapatite interfacial interaction. It shows that the tensile modulus of the system increase with the thickness, and it converges to a value that depends on  $k_3$ . Using the value of  $k_3$ , we can calculate the surface energy by using the linear assumption before bond breaking as  $\gamma_{sf} = k_3 \Delta x^2 / (2b\Delta l)$ . Panel b shows the relationship between the converged tensile modulus and the surface energy. On the basis of our results that show a converged tensile modulus is 30.16–31.87 GPa, and thereby from the result based on the elastic model, we can obtain the surface energy as 512.7–568.6 mJ/m<sup>2</sup> as indicated by the two highlighted points in the figure.

of the thinnest crystal (0.7 nm) is found to be about half of the convergence value. Also, in the case of the OH surface (dry conditions), the thickness has little or no influence, possibly due to the higher number of collagen–hydroxyapatite hydrogen bonds formed with respect to the Ca surface (see Figure 3). In the wet cases, the difference in the thickness effect (shown by  $E_\infty$  and  $h_0$ ) on the two surfaces is less strong, possibly due to the presence of water-mediated hydrogen bonds at the interface. This finding is supported by the evidence that water has a very strong attractive interaction with both the collagen and hydroxyapatite, especially for hydroxyapatite.<sup>39</sup> However, the existence of water can also have a function of decreasing direct mechanical connection between the tropocollagen molecule and hydroxyapatite. This has been shown in previous experimental works that investigated the effect of hydration in mineralized fibrils.<sup>5</sup> By comparing the deformation of the tissue, fibril, and mineral crystal level, it has been found that these three hierarchical levels take up successively lower levels of strain, in a ratio of 12:5:2. The reduced strain in the mineral particles relative to the fibril (5:2) means that the remaining three-fifths of the strain are likely transferred by shearing of the ductile collagen matrix. It is shown that the degree of hydration of the collagen matrix influences the amount of load on the mineral particles: dry collagen strains less, and hence the brittle mineral phase bears relatively more load. This result highlights the fact that in mineralized fibrils water has a lubricant effect, enhancing the shearing of collagen over hydroxyapatite and thus decreasing the direct coupling between collagen and mineral phase, which is consistent with our findings. Thus, by combining the analysis shown above to our simulation results of  $E_\infty$  for each surface, we can conclude that the existence of water mediates the collagen–hydroxyapatite interface, leading to a more uniform  $E$ – $h$  relationship for different surfaces as summarized in Table 2.

Using the similar technique as shown above for the tensile modulus, we investigate the tensile strength of the system for different surfaces and solvent conditions, which are summarized in Figure 5. We fit the maximum stress reached by the strain–stress curve as a function of the thickness by using

$$\sigma_C = \sigma_\infty - (\sigma_\infty - \sigma_{COL}) \exp(-h/h_\sigma) \quad (7)$$

where  $\sigma_\infty$  is the converged maximum stress,  $\sigma_{COL}$  (13 GPa from an earlier simulation study<sup>27</sup>) is the maximum stress of a pure tropocollagen molecule, and  $h_\sigma$  is the characteristic thickness. It shows that for hydroxyapatite crystals with a thickness beyond  $h_\sigma$ , increasing the thickness can only increase the strength of the system up to 15%. We summarize  $\sigma_\infty$  and  $h_\sigma$  for each of the two surfaces with and without water around the interface in Table 2. It can be seen that  $\sigma_\infty$  is rather insensitive on the surface or hydration state, reaching a value of  $\sim 20$  GPa. Similarly, we find a significant dependence on  $\sigma_C$  on  $h$  (shown for large  $h_\sigma$ ) for the Ca surface in dry condition. Also, in the case of OH surface (dry conditions), the thickness has little or no influence. In the wet cases, the difference in the thickness effect (shown by  $\sigma_\infty$  and  $h_\sigma$ ) is less strong for these two difference surfaces. This result agrees with the conclusion that the existence of water mediates the collagen–hydroxyapatite interface and leads to a more uniform  $\sigma_C$ – $h$  relationship for different surfaces. The result also indicates that since the tensile strength of the tropocollagen molecule is weaker than the collagen–hydroxyapatite composite, most of the rupture event happens by breaking the tropocollagen molecule instead of by breaking the interface, which is helpful for understanding the rupture mechanism in this composite material.

Our result shows that thin flakes of hydroxyapatite crystals with less than 1 nm can significantly improve the tensile modulus of the pure tropocollagen molecule. This observation is likely due to the fact that the tensile modulus of the hydroxyapatite is much higher than that of the tropocollagen molecule, making the composite much stiffer than pure collagen. This result agrees with experimental observations in which mineralized tendon shows a much higher tensile modulus (it can reach a factor of 10 times) than the unmineralized tendon.<sup>7</sup> However, the increment of the tensile modulus as a function of the hydroxyapatite thickness vanishes at less than 2 nm, which implies that thicker hydroxyapatite crystals do not further increase the tensile modulus beyond a characteristic size. However, further increasing the size of the mineral crystal may increase the brittleness of the collagen–hydroxyapatite composite. The convergence of the elastic properties is caused by the fact that increasing stiffness of the hydroxyapatite platelet with increasing thickness needs to conform with the stiffness of the tropocollagen molecule under



deformation through the collagen–hydroxyapatite interface that has its own effective stiffness. This result agrees to the observation that mineralized collagen structures in most forms of the natural morphology of bones are composed of collagen and thin hydroxyapatite flakes of a uniform size that varies between 1 and 4 nm in different bone types.<sup>7,40</sup> Such an agreement between simulations and experiments, even though only qualitative, given the difference in the actual structure of bone at the nanoscale, shows that the molecular structure of the collagen–hydroxyapatite interface is important in defining the mechanical and physiological properties of bone.

We ask the question: How can we explain the mechanical mechanism of this tensile modulus–thickness relationship, and how could we use our simulation results of the tensile modulus to quantitatively investigate the mechanical properties of the collagen–hydroxyapatite interface? We address the question by setting up an elastic network model of the collagen–hydroxyapatite interaction as illustrated in Figure 6b.<sup>41</sup>

As summarized in Figure 6a, as the thickness increases the tensile modulus of the system will increase, and it converges to a particular level as the increasing thickness does not contribute to further enhancing the tensile modulus. We also find that increasing in  $k_3$ , which represents all the nonbonded interactions (including the van der Waals interactions, the Coulomb interactions, and hydrogen bonds), leads to larger converged tensile modulus  $E_\infty$ . Using the value of  $k_3$ , we can calculate the surface energy by using the linear assumption before rupture of all the nonbonded interactions as  $\gamma_{sf} = k_3 \Delta x^2 / (2b\Delta l)$ , where  $\Delta x$  is the rupture distance of the adhesion force  $k_3$  at the interface, and we take its value to be the same as the cutoff length (1 nm) of nonbonded interaction we used in our simulations for reference. It is noted that this  $\Delta x$  has a different physical meaning from the cutoff in atomistic modeling because the cutoff in the atomistic modeling is a technique for the purpose of computational efficiency, but it should not affect the accuracy of atomic interactions, while for the elastic model this rupture distance corresponds to the maximum of chemical force at the interface. Although an increasing  $\Delta x$  leads to an increasing  $\gamma_{sf}$  for the elastic model, one cannot conclude that an increasing cutoff leads to a stronger interface (actually the surface energy for the atomistic model keeps constant for increasing cutoff beyond 1 nm). We study the relationship between the converged tensile modulus and the surface energy as shown in Figure 6b. It is shown that an increase in the surface energy leads to an increase in the converged tensile modulus, which corresponds to the maximum tensile modulus the system can reach by increasing the hydroxyapatite thickness. For our simulation result, we have seen that the converged tensile modulus is 30.16–31.87 GPa. Thus, from the result obtained using the elastic network model we obtain an estimate for the surface energy as 512.7–568.6 mJ/m<sup>2</sup>. This energy level is an order of magnitude higher than the gecko's hair adhesion energy on mineral surfaces, which is on the order of 50.0 mJ/m<sup>2</sup>,<sup>42</sup> the adhesion energy between vimentin protein and a silica surface of 36.7 mJ/m<sup>2</sup>,<sup>43</sup> as well as the adhesion energy of cells on a hydroxyapatite surface of 44.0 mJ/m<sup>2</sup>.<sup>44</sup> However, the energy level is an order lower than the adhesion energy between collagen molecules of three amino acids and hydroxyapatite ( $\sim 3000$  mJ/m<sup>2</sup>).<sup>24</sup> It is probably caused by the fact that the adhesion strength between tropocollagen and hydroxyapatite is stronger than other protein structures and other mineral surfaces, while the collagen molecule of three amino acids is free to adopt any conformation to be more

closely contacted with the hydroxyapatite surface, and thereby its adhesion energy is much higher than the tropocollagen case. It is also noted that the OH surface features a higher surface energy ( $\sim 50$  mJ/m<sup>2</sup>) than the Ca surface based on the higher converged tensile modulus as summarized in Table 2. This difference is likely caused by the fact that the chemical characteristic of the OH surface provides more donors and acceptors to form hydrogen bonds with collagen amino acids (as shown in Figure 3), which in return increase the interacting energy of the interface. The purpose of our elastic network model used here is to provide a tool to analyze experiment- and simulation-based data to estimate the surface energy by simply measuring the tensile modulus. To obtain a more accurate value of the collagen–hydroxyapatite interaction energy, we could, in principle, also use the atomic model with actual collagen amino acid sequence information and measure the free energy landscape by metadynamics simulations for all the nonbonded interactions.

#### 4. CONCLUSION

Here we systematically studied the effect of mineral surface, mineral thickness, and hydration state on the mechanical properties of a collagen–mineral interface. We found that increasing the thickness of the mineral crystal increases the tensile modulus of the biomineral surface, in particular for the Ca surface. On the other hand, the tensile modulus of the biomineral interface does not depend on the surface and hydration state, reaching a value of  $\sim 31$  GPa for increasing thicknesses. Specifically, the tensile modulus converges at a thickness of less than 2 nm, which agrees with experimental observations that the hydroxyapatite nanocrystals in bone are typically very thin flakes with 1–2 nm thicknesses. Our simulation results also show that the existence of water mediates the tensile modulus and strength of the collagen–hydroxyapatite interface, leading to more uniform tensile modulus–thickness and tensile strength–thickness relationships for different hydroxyapatite surfaces with different chemical compositions. This result implies that the mechanical properties of bone are governed by the molecular structure at the collagen–hydroxyapatite interface. In turn, the microscopic structure of bone has evolved in nature largely according to its mechanical requirement to achieve its crucial function in supporting and protecting the body. Our work provides a systematic quantification of the mechanical properties of the collagen–hydroxyapatite interface, one of the most important biomineral composites. This work could be further extended to study the effect of collagen mutations on the interface properties, helping to understand the origins of collagen related diseases such as osteogenesis imperfecta (brittle bone disease).

#### ■ AUTHOR INFORMATION

##### Corresponding Author

\*Electronic address: mbuehler@MIT.EDU. Phone: +1-617-452-2750. Fax: +1-617-324-4014.

#### ■ ACKNOWLEDGMENTS

We acknowledge support from AFOSR, ONR-PECASE, MIT-Italy Program (“Progetto Rocca”) and Politecnico di Milano (Grant “5 per mille junior 2009”). High-performance computing resources have been provided by Regione Lombardia and CILEA Consortium through the LISA Initiative and by CINECA under the ISCRA initiative. H.I. acknowledges

support from Weizmann Institute of Science (Israel), support from the Center for Excellence in Education, as well as the Research Science Institute (RSI).

## REFERENCES

- (1) Currey, J. D. *Bones: Structure and Mechanics*; Princeton University Press: Princeton, NJ, 2002.
- (2) Fratzl, P.; Weinkamer, R. Nature's hierarchical materials. *Prog. Mater. Sci.* **2007**, *52*, 1263–1334.
- (3) Fratzl, P. *Collagen: Structure and Mechanics*; Springer: New York, 2008.
- (4) Fratzl, P.; Gupta, H. S.; Paschalis, E. P.; Roschger, P. Structure and mechanical quality of the collagen-mineral nano-composite in bone. *J. Mater. Chem.* **2004**, *14* (14), 2115–2123.
- (5) Gupta, H. S.; Seto, J.; Wagermaier, W.; Zaslansky, P.; Boesecke, P.; Fratzl, P. Cooperative deformation of mineral and collagen in bone at the nanoscale. *Proc. Natl. Acad. Sci. U.S.A.* **2006**, *103* (47), 17741–17746.
- (6) Jager, I.; Fratzl, P. Mineralized collagen fibrils: A mechanical model with a staggered arrangement of mineral particles. *Biophys. J.* **2000**, *79* (4), 1737–1746.
- (7) Weiner, S.; Wagner, H. D. The material bone: Structure mechanical function relations. *Annu. Rev. Mater. Sci.* **1998**, *28*, 271–298.
- (8) Ji, B. H.; Gao, H. J. Mechanical properties of nanostructure of biological materials. *J. Mech. Phys. Solids* **2004**, *52* (9), 1963–1990.
- (9) de Leeuw, N. H. Local ordering of hydroxy groups in hydroxyapatite. *Chem. Commun.* **2001**, *17*, 1646–1647.
- (10) Hauptmann, S.; Dufner, H.; Brickmann, J.; Kast, S. M.; Berry, R. S. Potential energy function for apatites. *Phys. Chem. Chem. Phys.* **2003**, *5* (3), 635–639.
- (11) Snyders, R.; Music, D.; Sigumonrong, D.; Schelnberger, B.; Jensen, J.; Schneider, J. M. Experimental and ab initio study of the mechanical properties of hydroxyapatite. *Appl. Phys. Lett.* **2007**, *90*, 19.
- (12) Ching, W. Y.; Rulis, P.; Misra, A. Ab initio elastic properties and tensile strength of crystalline hydroxyapatite. *Acta Biomater.* **2009**, *5* (8), 3067–3075.
- (13) Cruz, F. J. A. L.; Canongia Lopes, J. N.; Calado, J. C. G.; Minas da Piedade, M. E. A molecular dynamics study of the thermodynamic properties of calcium apatites. 1. Hexagonal phases. *J. Phys. Chem. B* **2005**, *109* (51), 24473–24479.
- (14) Zhang, H.-p.; Lu, X.; Leng, Y.; Fang, L.; Qu, S.; Feng, B.; Weng, J.; Wang, J. Molecular dynamics simulations on the interaction between polymers and hydroxyapatite with and without coupling agents. *Acta Biomater.* **2009**, *5* (4), 1169–1181.
- (15) Zhou, H.; Wu, T.; Dong, X.; Wang, Q.; Shen, J. Adsorption mechanism of BMP-7 on hydroxyapatite (001) surfaces. *Biochem. Biophys. Res. Commun.* **2007**, *361* (1), 91–96.
- (16) Shen, J.-W.; Wu, T.; Wang, Q.; Pan, H.-H. Molecular simulation of protein adsorption and desorption on hydroxyapatite surfaces. *Biomaterials* **2008**, *29* (5), 513–532.
- (17) Bhowmik, R.; Katti, K. S.; Katti, D. R. Mechanisms of load-deformation behavior of molecular collagen in hydroxyapatite-tropocollagen molecular system: Steered molecular dynamics study. *J. Eng. Mech.* **2009**, *135* (5), 413–421.
- (18) Bhowmik, R.; Katti, K. S.; Katti, D. R. Mechanics of molecular collagen is influenced by hydroxyapatite in natural bone. *J. Mater. Sci.* **2007**, *42* (21), 8795–8803.
- (19) Almora-Barrios, N.; de Leeuw, N. H. Modelling the interaction of a Hyp-Pro-Gly peptide with hydroxyapatite surfaces in aqueous environment. *CrystEngComm* **2010**, *12* (3), 960–967.
- (20) de Leeuw, N. H.; Almora-Barrios, N. A density functional theory study of the interaction of collagen peptides with hydroxyapatite surfaces. *Langmuir* **2010**, *26* (18), 14535–14542.
- (21) Dubey, D. K.; Tomar, V. Role of the nanoscale interfacial arrangement in mechanical strength of tropocollagen–hydroxyapatite-based hard biomaterials. *Acta Biomater.* **2009**, *5* (7), 2704–2716.
- (22) Dubey, D. K.; Tomar, V. Role of hydroxyapatite crystal shape in nanoscale mechanical behavior of model tropocollagen–hydroxyapatite hard biomaterials. *Mater. Sci. Eng. C: Mater. Biol. Appl.* **2009**, *29* (7), 2133–2140.
- (23) Zahn, D.; Duchstein, P. Atomistic modeling of apatite-collagen composites from molecular dynamics simulations extended to hyperspace. *J. Mol. Model.* **2011**, *17* (1), 73–79.
- (24) Almora-Barrios, N.; de Leeuw, N. H. A density functional theory study of the interaction of collagen peptides with hydroxyapatite surfaces. *Langmuir* **2010**, *26* (18), 14535–14542.
- (25) Rainey, J. K.; Goh, M. C. An interactive triple-helical collagen builder. *Bioinformatics* **2004**, *20* (15), 2458–9.
- (26) Gautieri, A.; Buehler, M. J.; Redaelli, A. Deformation rate controls elasticity and unfolding pathway of single tropocollagen molecules. *J. Mech. Behav. Biomed. Mater.* **2009**, *2* (2), 130–7.
- (27) Buehler, M. J. Atomistic and continuum modeling of mechanical properties of collagen: Elasticity, fracture and self-assembly. *J. Mater. Res.* **2006**, *21* (8), 1947–1961.
- (28) Gautieri, A.; Buehler, M. J.; Redaelli, A. Deformation rate controls elasticity and unfolding pathway of single tropocollagen molecules. *J. Mech. Behav. Biomed. Mater.* **2009**, *2* (2), 130–137.
- (29) Brooks, B. R.; Bruccoleri, R. E.; Olafson, B. D.; States, D. J.; Swaminathan, S.; Karplus, M. CHARMM - A program for macromolecular energy, minimization, and dynamics calculations. *J. Comput. Chem.* **1983**, *4* (2), 187–217.
- (30) Park, S.; Radmer, R. J.; Klein, T. E.; Pande, V. S. A new set of molecular mechanics parameters for hydroxyproline and its use in molecular dynamics simulations of collagen-like peptides. *J. Comput. Chem.* **2005**, *26* (15), 1612–1616.
- (31) Gautieri, A.; Uzel, S.; Vesentini, S.; Redaelli, A.; Buehler, M. J. Molecular and mesoscale mechanisms of osteogenesis imperfecta disease in collagen fibrils. *Biophys. J.* **2009**, *97* (3), 857–865.
- (32) Gautieri, A.; Vesentini, S.; Redaelli, A.; Buehler, M. J. Hierarchical structure and nanomechanics of collagen microfibrils from the atomistic scale up. *Nano Lett.* **2011**, *11* (2), 757–766.
- (33) Bhowmik, R.; Katti, K. S.; Katti, D. Molecular dynamics simulation of hydroxyapatite–polyacrylic acid interfaces. *Polymer* **2007**, *48* (2), 664–674.
- (34) Plimpton, S. Fast parallel algorithms for short-range molecular dynamics. *J. Comput. Phys.* **1995**, *117* (1), 1–19.
- (35) Gautieri, A.; Vesentini, S.; Redaelli, A.; Buehler, M. J. Intermolecular slip mechanism in tropocollagen nanofibrils. *Int. J. Mater. Res.* **2009**, *100* (7), 921–925.
- (36) Srinivasan, M.; Uzel, S. G. M.; Gautieri, A.; Ketten, S.; Buehler, M. J. Alport Syndrome mutations in type IV tropocollagen alter molecular structure and nanomechanical properties. *J. Struct. Biol.* **2009**, *168* (3), 503–510.
- (37) Qin, Z.; Kreplak, L.; Buehler, M. J. Hierarchical structure controls nanomechanical properties of vimentin intermediate filaments. *PLoS ONE* **2009**, *4* (10), e7294.
- (38) Humphrey, W.; Dalke, A.; Schulten, K. VMD: Visual molecular dynamics. *J. Mol. Graph.* **1996**, *14* (1), 33–38.
- (39) Katti, D. R.; Pradhan, S. M.; Katti, K. S. Directional dependence of hydroxyapatite–collagen interactions on mechanics of collagen. *J. Biomech.* **2010**, *43* (9), 1723–1730.
- (40) Hu, Y. Y.; Rawal, A.; Schmidt-Rohr, K. Strongly bound citrate stabilizes the apatite nanocrystals in bone. *Proc. Natl. Acad. Sci. U.S.A.* **2010**, *107* (52), 22425–22429.
- (41) Qin, Z.; Buehler, M. J. Cooperative deformation of hydrogen bonds in beta-strands and beta-sheet nanocrystals. *Phys. Rev. E* **2010**, *82*, 6.
- (42) Prowse, M. S.; Wilkinson, M.; Puthoff, J. B.; Mayer, G.; Autumn, K. Effects of humidity on the mechanical properties of gecko setae. *Acta Biomater.* **2011**, *7* (2), 733–738.
- (43) Kirmse, R.; Qin, Z. A.; Weinert, C. M.; Hoenger, A.; Buehler, M. J.; Kreplak, L. Plasticity of intermediate filament subunits. *PLoS ONE* **2010**, *5*, 8.
- (44) Redey, S. A.; Razzouk, S.; Rey, C.; Bernache-Assollant, D.; Leroy, G.; Nardin, M.; Cournot, G. Osteoclast adhesion and activity

on synthetic hydroxyapatite, carbonated hydroxyapatite, and natural calcium carbonate: relationship to surface energies. *J. Biomed. Mater. Res.* **1999**, *45* (2), 140–7.

(45) Sun, Y. L.; Luo, Z. P.; Fertala, A.; An, K. N. Stretching type II collagen with optical tweezers. *J. Biomech.* **2004**, *37* (11), 1665–1669.

(46) Gilmore, R. S.; Katz, J. L. Elastic properties of apatites. *J. Mater. Sci.* **1982**, *17* (4), 1131–1141.